Thermal Analysis of Foil Wound Concentrated Coils for Use in Axial Flux Permanent Magnet Alternators

Supported by the Austrian Marshall Plan Foundation

Under the supervision of Professor Annette Mütze at the Graz University of Technology

Submitted on 13 November 2015

By Michael Rios

Table of Contents

I. ABSTRACT 3

II. INTRODUCTION 3

III. MOTIVATION 4

IV. LITERATURE REVIEW 7

Axial Flux Permanent Magnet Alternators 7

Foil Windings in Electric Machines 8

Analytical Thermal Modeling 9

AC Losses in Stator Windings 10

V. EXPERIMENT DESIGN 10

Experiment 1: Temperature Distribution in Concentrated Coil 11

Experiment 2: Single Axis Heat Transfer in Concentrated Coil 16

Radial (X-Axis) Heat Flow 16

Axial (Y-Axis) Heat Flow 17

VI. ANALYTICAL MODEL 20

Three Layer Analytical LP Thermal Model Example 22

VII. RESULTS 28

Observation 1: LP Model Predicts Temperature Distribution in Foil 28

Observation 2: Foil Conductor vs Round Conductor 29

Observation 3: Double-Sided Nomex Paper Insulation vs Single-Sided PET Insulation 30

Observation 4: Foil on Stator vs Round Conductor on Bobbin 31

Observation 5: Stator Apparatus vs Plastic Bobbin 32

Observation 6: Vertical vs Horizontal Coil Orientation 34

Summary 35

VIII. CONCULUSIONS AND FUTURE WORK 35

Future Work - Preliminary Exam Outline 37

IX. ACKNOWLEDGEMENTS 39

X. REFERENCES 39

I. ABSTRACT

Axial flux permanent magnet (AFPM) generators for small-scale wind turbine applications have proven to be a useful design due to their reliability and ease of construction. Their stators have been realized using concentrate coils of enameled copper wires embedded in an epoxy-resin composite mixture. A static setting, opposed to a dynamic machine environment, is utilized to study the steady state thermal properties of five different variations of a single concentrated coil. This study was conducted to better understand the heat transfer properties, as well as verify other claims that foil windings have superior thermal characteristics over their round conductor counterpart.

II. INTRODUCTION

Although foil windings have been used in transformers and air core inductors, they have rarely been used in modern electric machines. There is an increasing demand for electric machines to play a larger role in a variety of industries. Electric machines boast a high efficiency and control sophistication which makes them an attractive alternative for many applications where mechanical power, in one form or another, is required. Notably in the aerospace industry there is a call for a more electric aircraft to reduce weight and improve reliability. Traditional pneumatic and hydraulic systems, however, offer power densities that remain difficult to match for electric machines. Axial flux machines have several advantages to their radial flux machine counterparts, especially in terms of power density. However, both radial and axial flux machines that exhibit high power densities are consequently subjected to a high temperature environment. As a result, high power density electric machines have many thermal related failures, particularly in the stator windings. Thermal issues for electric machines have been recognized both in industry and academia, but the investigations are typically application specific. This novel foil winding approach demands a more comprehensive study. In order to isolate the steady state thermal properties of a concentrated coil, a static setting, as opposed to a dynamic machine environment, is used. A variety of concentrated coils are constructed to create a comparative study between different coil winding designs. Specifically, a baseline design of a standard copper round conductor

magnet wire will be compared against different copper foil winding configurations. Two experiments are conducted to determine the temperature variation over an increasing DC current input. Additionally, an analytical lumped parameter (LP) model is developed to obtain a fast and accurate overview of the thermal behavior of the foil wound concentrated coils. Isolating the windings can help to identify a more intelligent winding configuration when designing for electric machines. The proposed project develops a better thermal model of a novel foil winding design for use in electric machines. The enhanced model will facilitate innovations that will improve the thermal performance and overall reliability for electric machines.

The following section describes the inspiration behind this research topic to study foil wound concentrated coils for use in electric machines. Section IV is a survey of the literature that discusses the AFPM machines, the use of foil windings in electric machines, analytical thermal modeling of electric machines, and AC winding losses. Section V describes the two experiments conducted. Section VI details the analytical LP model developed to characterize the thermal behavior of the concentrated coils. Section VII presents conclusive results of the aforementioned experiments and analytical model. Section VIII discusses the conclusions and future work, which will carry on to the PhD dissertation. And the final sections, Acknowledgements and References provide additional reference information for the reader.

III. MOTIVATION

The motivation to study foil wound concentrated coils for use in electric machines stemmed from previous work done at the University of Wisconsin that involved using Aluminum foil concentrated windings in a small-scale axial flux permanent magnet (AFPM) wind turbine. This work is summarized in [1] and describes unique methodologies for the design and fabrication of the stator and blades of a small scale wind turbine. Different methodologies promote different manufacturing procedures that reduce the time and skills needed to manufacture small scale wind turbines, as well as utilizing low-cost readily available materials for the components, such as Aluminum. The most expensive parts of the described wind turbine is the coils and magnets, so working

to reduce the amount of copper or permanent magnet (PM) material would significantly reduce the cost.

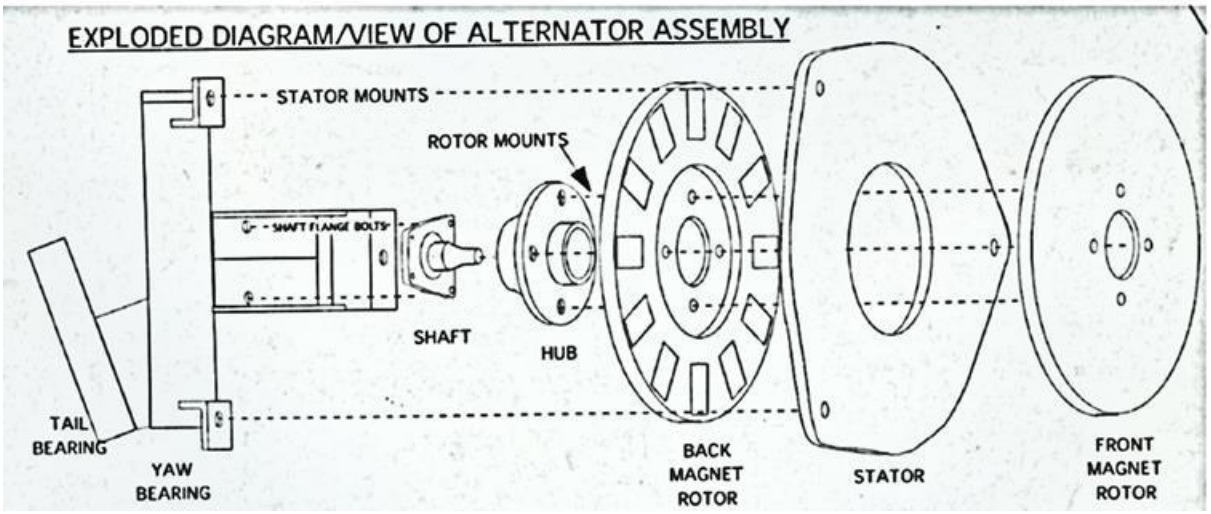

Figure 1 Double Sided Rotor AFPM Wind Turbine Assembly

The system design is a simple tower mounted generator with a furling tail to direct the blades into the wind at low wind speeds for harvesting maximum possible power and direct the blades out of the wind at high speeds for protection [2]. The wind turbine is a 3-blade, direct-drive (no gearbox) design. This design is ideal since they require a low starting torque and can extract the maximum amount of energy at low speeds [3]. The turbine uses an AFPM machine using concentrated-coil embedded in air-cored stators, which does not have the problem of cogging torque credited to the absence of iron in the stator [4]. Maximum power is about 500 W at rated conditions. The alternator feeds into a passive diode rectifier, which charges sealed lead acid batteries for energy storage. The design uses a double sided rotor construction, with the two rotors consisting of an 8mm thick, 300mm diameter steel plate with 12 NdFeB magnets cast in epoxy-resin composite [1]. The magnets are evenly spaced on an iron round rotor and embedded in a resin cast to protect the magnets from corrosion. The stator consists of 10 coils divided into 5 phases, of two coils each. In the baseline design, each coil has 150 turns of 0.8mm diameter enamel copper; its inner window is sized to fit the surface area of the magnets, which are 30mm x 46mm. The axial thickness of the coil is 13mm, which defines the minimum air gap length, which excludes the mechanical clearance

[1]. The 12 magnet poles traverse the coils at different instants of time, creating a phase lag between the coils [3]. The phase lag reduces vibrations and allows for smoother rotation. A simplified schematic of the magnetic circuit for one pole pair of the AFPM alternator is shown in Figure 1.

Among the innovations that resulted from this thesis was the use of aluminum foil wound concentrated coils in the air-cored stator. Three aluminum prototype coils were constructed (AP-1, AP-2, and AP2-2), tested, and compared to the baseline copper design. Figure 2 shows that the aluminum prototype coils are comparable to the copper baseline design. This is an impressive result considering the superior electrical characteristics of copper conductors. It begs to question if the aluminum prototypes perform so well due to their foil geometry or due to the fact that they are insulated by VHS tape, which reduces the reluctance of the air gap across the coil.

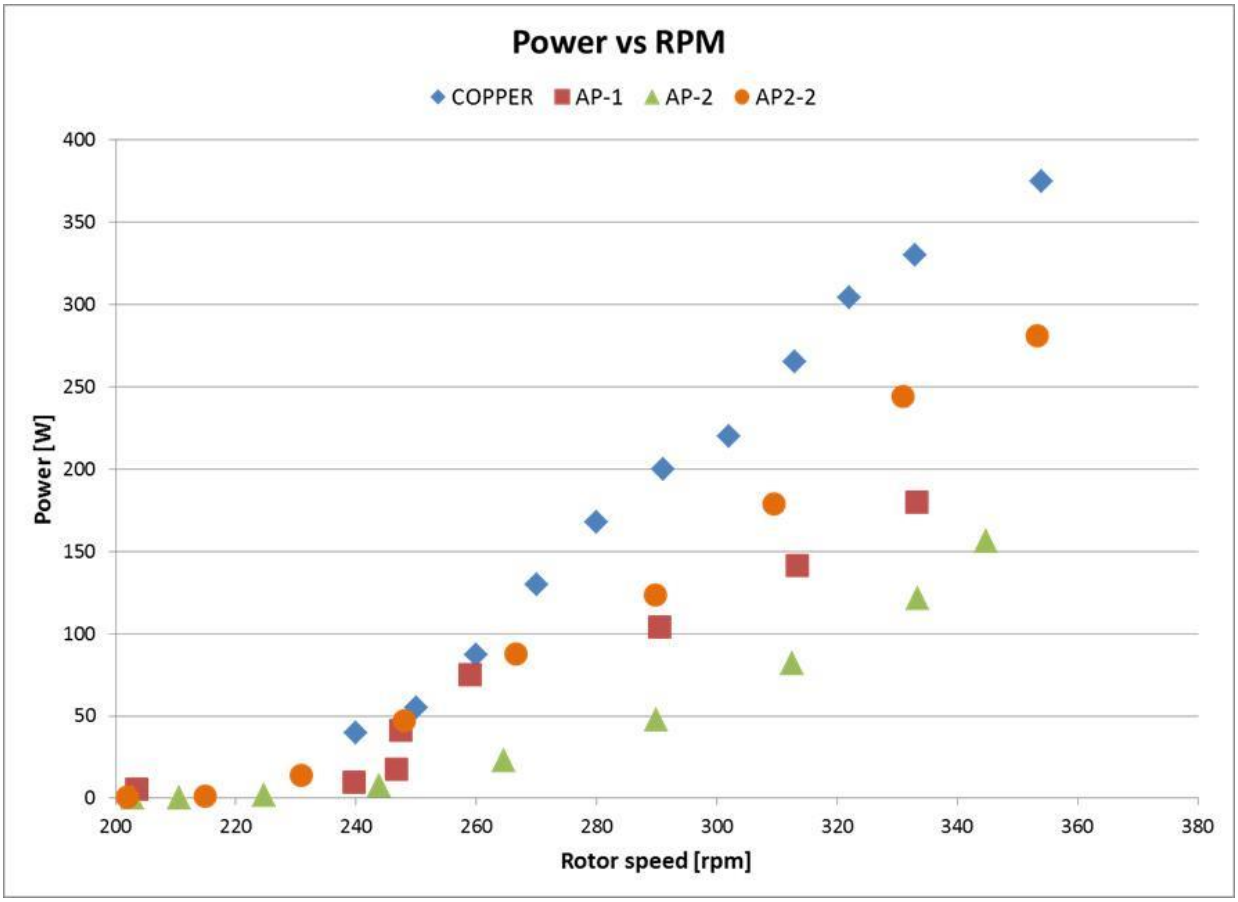

Figure 2 Generated Power-Speed Curve for All Coil Designs

It is well known that foil conductors have a superior fill factor to their round conductor counterpart but what other advantages can come from using a foil wound concentrate coil? Thus it was determined that a thorough study of foil wound concentrated coils was necessary to understand the design trade-offs and permit the use of foil conductors for use in electric machines.

IV. LITERATURE REVIEW

The literature pertinent to this study covers the topic of AFPM alternators, foil or non-cylindrical conductors in electric machines, analytical thermal modeling techniques, and AC losses in windings. The literature that outlines the AFPM topology provides insight to the background of the project. Following the use of foil windings in [1], other literature indicates a trend toward nontraditional conductors in electric machines. The main content of this study involves experiments on the topic of thermal modeling. Lastly, there is brief mention of AC losses in conductors, which provides an appropriate bridge to the future work of the study of non-cylindrical conductors for use in electric machines.

Axial Flux Permanent Magnet Alternators

Axial flux permanent magnet alternators are most often found in the context of small-scale wind turbine designs due to relatively simple construction guide outlined by Hugh Piggott [3]. Piggott provides the necessary information to build an AFPM alternator, detailed above in the Motivation section above, including how to carve wooden turbine blades and how to construct the PM alternator. The alternator can be seen in Figure 1 as a two-sided PM rotor with the resin-casted stator between the rotor plates. As previously mentioned, researchers at the University of Wisconsin studied the simple design that Piggott provided and sought to bring innovation to the overall system. Reed discusses the mechanical furling mechanism used to protect the turbine apparatus in high speed winds and how to use the AFPM alternator as a source for a battery charging [2]. Melendez-Veg, presents innovations on both the blades and the stator design [1]. The use of aluminum for the stator windings promotes using a more sustainable and cheaper metal. And the use of Video Home System (VHS) tape as the insulation for the concentrated coils promote recycling electronic waste while simultaneously resulting in reduced reluctance of the large air gap. These key

innovations in the prototype stator windings in [1] have two unique features: the aluminum foil wound concentrated coils and the VHS tape used to insulate the concentrated coil. The first feature is the topic of this paper. The second feature is discussed in [7]. Shea investigates the use of minimal iron in the otherwise ironless air gap in order to reduce the large reluctance of the air gap with minimal cogging torque. This is an important feature because it allows for further cost reduction by reducing the amount of PM material necessary in the rotor plates. For the Piggott AFPM alternator, the PM material amounts to about 36% of the total turbine alternator material cost [7]. Shea is able to reduce the total amount of PM material by 50% while maintaining, or enhancing, electrical performance with a reasonable amount of cogging torque [7]. Kamper provides a more traditional study for AFPM machines with air-cored concentrated coils [4]. Kamper finds that despite the fact that concentrated windings have a lower winding factor than overlapping windings, they can have similar performance. Other advantages to using a AFPM concentrated coil machine is that there is less copper mass compared to overlapping windings and the voltage waveform generated has a very clean sinusoidal output due to the absence of any cogging torque.

Foil Windings in Electric Machines

Melendez-Vega's main ambition was to find a way to reduce the cost of the raw materials needed to construct an AFPM alternator, and that was achieved with the aluminum foil concentrated coils. Although foil conductors are more commonly found in transformers, there are various papers that support the trend of using foil conductors in electric machines. Lorilla uses foil for a field winding in a Lundell alternator, which boasts a higher packing factor and improved heat transfer properties [8]. A 15% improved packing factor with the copper foil field winding is cited [8]. Babicz tests anodized aluminum foil windings for use in electric machines, stating advantages in packing factor, thermal characteristics, and a cheaper and lighter machine [9]. Another advantage to being able to use aluminum for machine windings is aluminum has a high melting point, at approximately 660˚ Celsius. Babicz also supports the idea that the foil shape is better suited to transfer heat. Arumugam uses foil windings for a stator stating that the foil windings, or "vertical strip windings," reduces the dependence on the position of a fault within the slot of the PM synchronous motor [5], [6]. Another important

find in [6] is that when the original round conductors are replaced by the vertical strip windings the losses in the strip windings are significantly higher than the round conductors. However, Arumugam claims that when the machine is designed to cater to the shape of the vertical strip windings, per the tooth-width/slot pitch ratio, the losses in the vertical strip windings can be significantly reduced. This is important finding when considering the future direction of foil wound concentrated coils in electric machines. There is also indication of using other non-cylindrical type windings, like for wound windings. Lomheim uses customized formed solid copper windings for the stator in an AFPM motor for a high torque motor application [10]. Wojciechowski and Zhang both study various orientations of rectangular conductors in a slot, but more in the context of AC losses, which will be discussed later [20], [21].

Analytical Thermal Modeling

Thermal modelling of electric machines is a large field that has been studied extensively. Thermal models for machines may take the form of LP models, finite-element analysis, or computational fluid dynamics [12], but this report will focus solely on LP analytical modeling. Thermal circuit models, or LP thermal models, provide a fast, accurate way to determine the temperature distribution in an electric machine [14], [16]. However, stator windings are often reduced to one node in the LP model of the electric machine. Even Boglietti claims that it is not necessary to model each individual conductor to accurately predict the temperature distribution of the windings [11]. But Boglietti acknowledges that the stator windings are indeed a critical parameter when building a thermal model for a machine. The specific critical parameters are listed as: the equivalent thermal resistance between external frame and ambient at zero fan speed, equivalent thermal conductivity between winding and lamination, forced convection heat transfer coefficient between end winding and end-caps, the radiation heat transfer coefficient between external frame and ambient, the interface gap between lamination and external frame, air cooling speed, and the bearing equivalent thermal resistance [11]. If the stator slots are an area of interest it is important to consider the slot liner, wire insulation, impregnation, slot contact, and air gap convection [11], [13]. Sensitivity analysis can be performed to determine which parameters are the most important for a given application. Simpson and Wrobel conduct heat flow studies to

calculate precise heat transfer coefficient, which is essential for parameter estimation of impregnated windings in electric machines [17], [18].

AC Losses in Stator Windings

Although the topic of AC losses in stator windings is not studied in this report it is the next crucial step in the study of foil wound concentrated coils. Kheraluwala does not specifically study foil conductors in electric machines but it does bring up the concern of induced eddy currents in the larger surface area that defines foil conductors [19]. Zhang shows that the number of conductors in each slot and their dimensions can have a significant impact on how the skin and proximity losses arise in higher frequency excitations [20]. This is further verified by Wojciechowski, who investigates the use of foil, or “tape,” wound concentrated windings for PM synchronous motors [21]. Lammeraner and Stafl provide the mathematical framework necessary to study eddy currents, in the scope of electric machines [22].

V. EXPERIMENT DESIGN

The experiment design phase followed the literature review and resulted in experiment proposals to study the steady state heat transfer characteristics of the concentrated coils. The first proposed experiment was based on [17] where an impregnated cut sample of the proposed winding is placed between a hot plate and a cold plate, see Figure 3. This allows the heat transfer characteristics of the sample to be studied in one axis at a time. However, the experimental setup is complex and it is distinctly different in that the heat generation occurs at the boundary of the hot plate, as opposed to within each individual layer of the concentrated coil. This led to the decision to conduct the thermal experiments using a DC current source to feed the concentrated coil, relying on the copper losses to act as an internal heat source for each conductor layer.

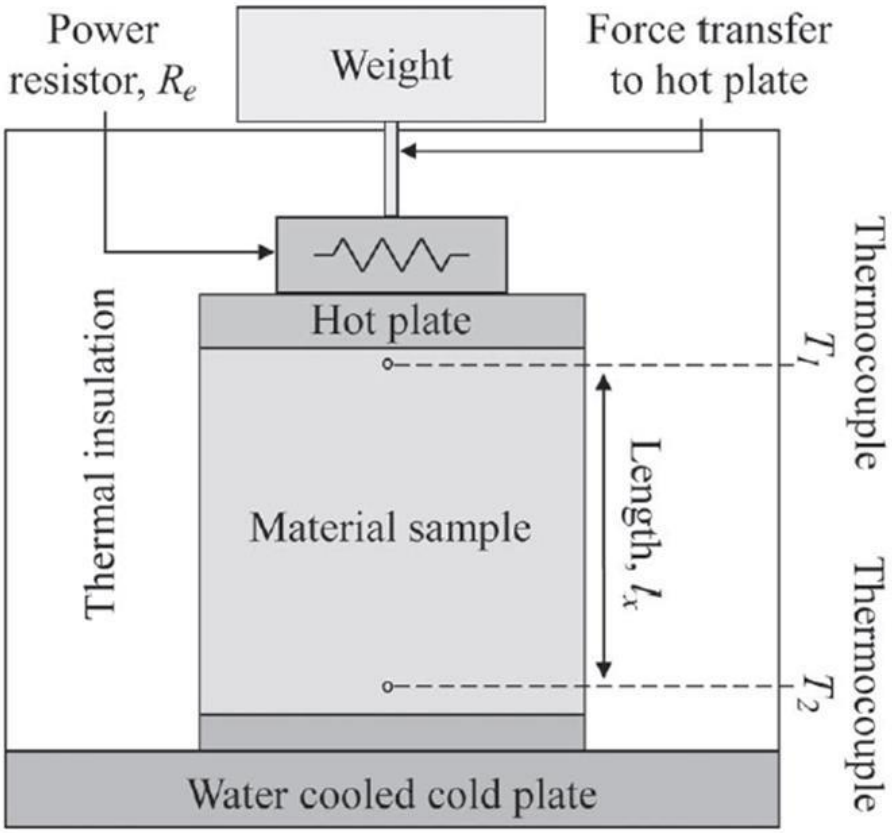

Figure 3 Hot/Cold Plate Heat Flow Meter Experiment [17]

Two experiments are designed to study the heat transfer characteristics of five different concentrated coils. The first experiment uses a DC current input with five different concentrated coils and measures the steady state temperature in three distinct spots. The second experiment uses Styrofoam to insulate part of the concentrated coil so that the heat transfer in a single axis of the coil can be observed.

Experiment 1: Temperature Distribution in Concentrated Coil

The experimental setup consists of five concentrated coils with embedded temperature probes, each subjected to a constant DC current source at varying levels. The five coils are subject to nine operating points: 1A, 1.5A, 2A, 2.5A, 3A, 3.5A, 4A, 4.5A, and 5A. The parameters of the five concentrated coils that were constructed for the experiment can be found in Table 1. Figure 4 is a legend used to define the coil names seen in Table 1, and which will be referenced throughout the paper.

Three thermistors are used to measure the temperature: one within the last ten turns, one in the middle, and one within the first ten turns, the “outside,” “middle,” and “inside,” temperatures respectively. The temperature probe placement can be seen best in Figure 7. Thermistors are used because they are easy to use, cheap, and very sensitive to changes in temperature. Since thermistors produce a nonlinear voltage they are generally best suited for applications that under 100° Celsius [19]. Additionally, a Keithley 2700 multimeter is used for temperature measurements, which is equipped with twenty thermistor inputs and has built-in default settings for 10kΩ thermistors.

All of the coils are wound by hand around a square plastic bobbin, with the exception of one coil which is wound around a solid stainless steel “stator” tooth. The winding apparatuses are necessary to maintain the structure of the concentrated coil. Figure 5 is a 3D illustration of the stainless steel stator winding apparatus and Figure 6 shows coil A1S150N around the middle tooth of the “stator” structure. Figure 7 and Figure 8 illustrate coils A1B85N and A2B150E, respectively, around a plastic bobbin.

Following the construction of the various concentrated coils, a DC current source is connected to the device under test. An ammeter is connected in series with the current source to have an accurate measurement of the current that is being fed through the coil. Also, a voltage meter is used to measure the voltage drop across the concentrated coil. Thus, the cold and hot resistance of the coil can be determined. The change in resistance is linearly proportional to the linear change in temperature. So the average coil temperature can be found from the resistance change. At each operating point, the thermistors and coil resistance had to reach a steady state value, which often took about two hours.

A1/A2	S/B	150/85	N/P/E
Cross-sectional Area	Winding Apparatus	Number of Turns	Insulation Type

Figure 4 Concentrated Coil Name Legend

Table 1 Concentrated Coil Parameters

Coil Name	A1S150N	A1B85N	A2B150N	A2B150E	A2B150P
Number of Turns	150	85	150	150	150
Conductor Width [mm]	12.7	12.7	13.005	1.12	13.0048
Conductor Thickness [mm]	0.0508	0.0508	0.0762	N/A	0.0762
Conductor Cross Sectional Area [mm2]	0.645	0.645	0.991	0.985	0.991
Winding Apparatus	Stainless Steel "Stator"	Plastic Bobbin	Plastic Bobbin	Plastic Bobbin	Plastic Bobbin
Insulation Type	Two-Sided Nomex Paper	Two-Sided Nomex Paper	Two-Sided Nomex Paper	Enamel	One-Sided PET
Insulation Width [mm]	15.875	15.875	17.145	N/A	17.145
Insulation Thickness [mm]	0.0508	0.0508	0.03048	0.0381	0.03048

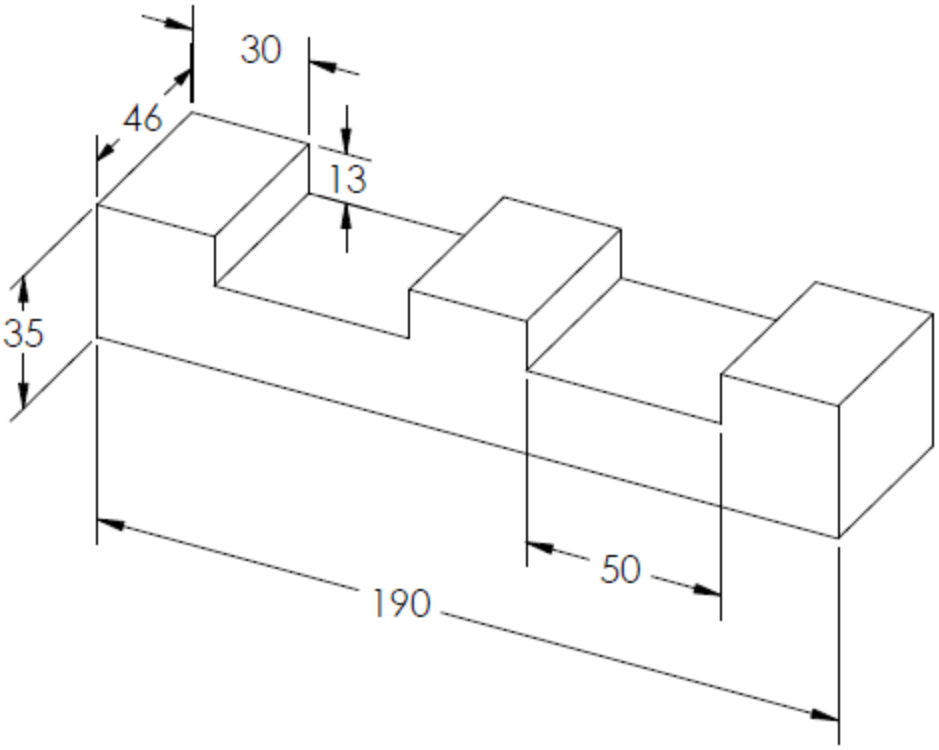

Figure 5 "Stator" Winding Apparatus Drawing

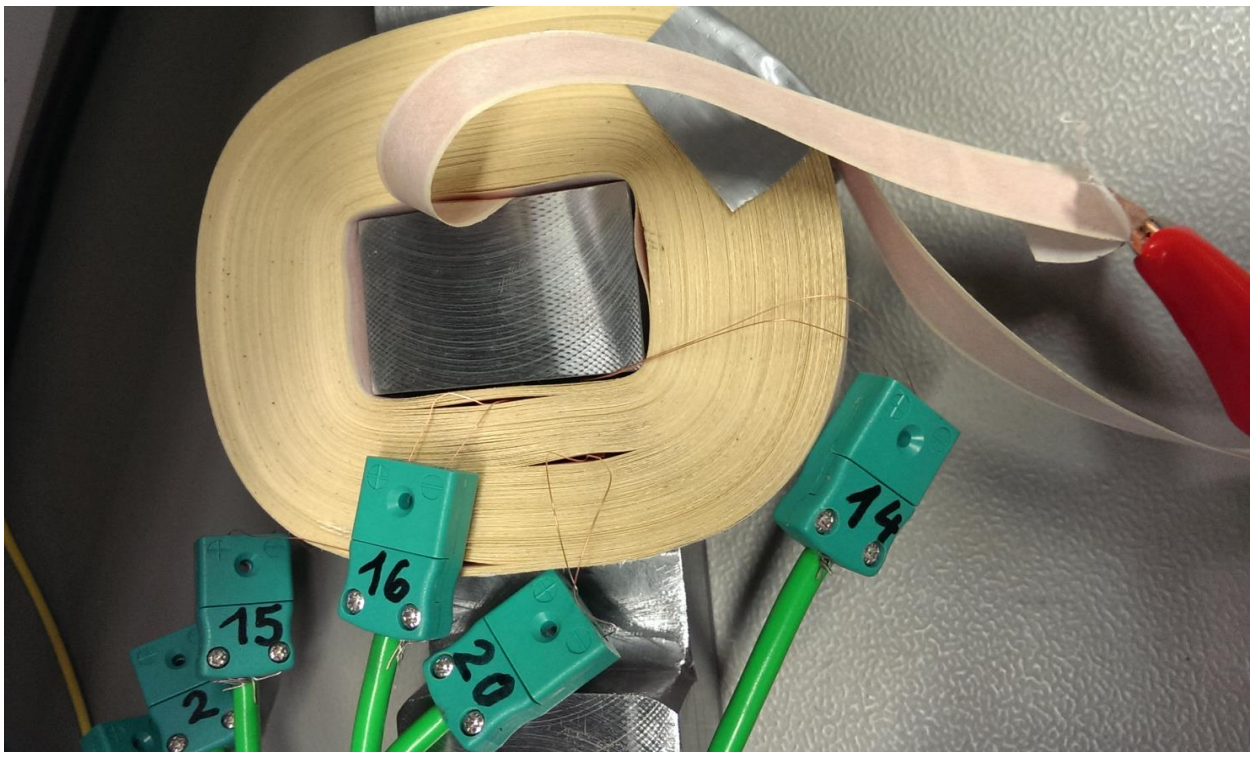

Figure 6 A1S150N Coil on Stainless Steel "Stator"

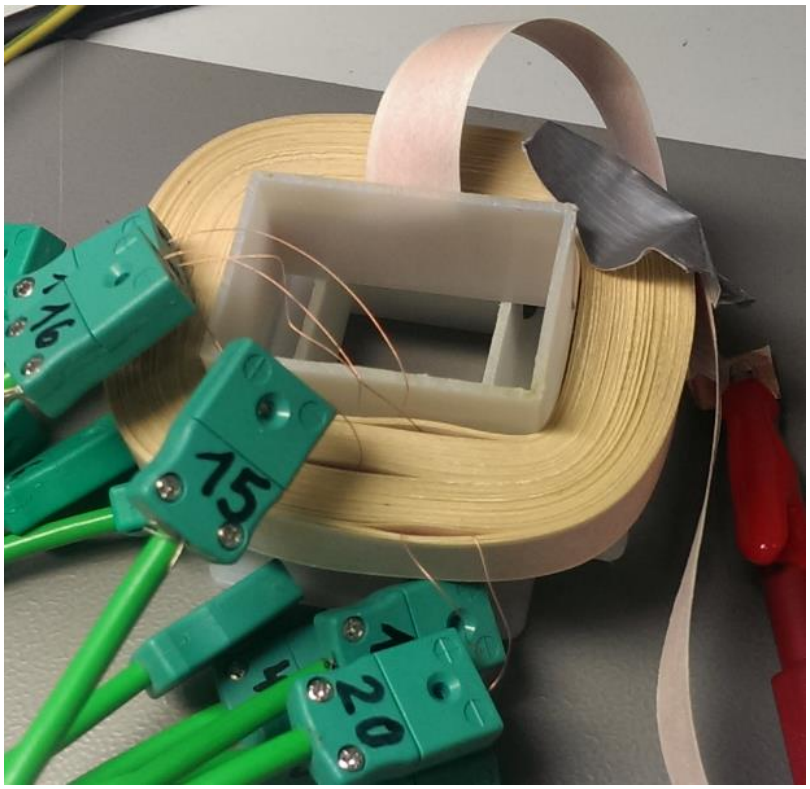

Figure 7 A1B85N Coil on Plastic Bobbin

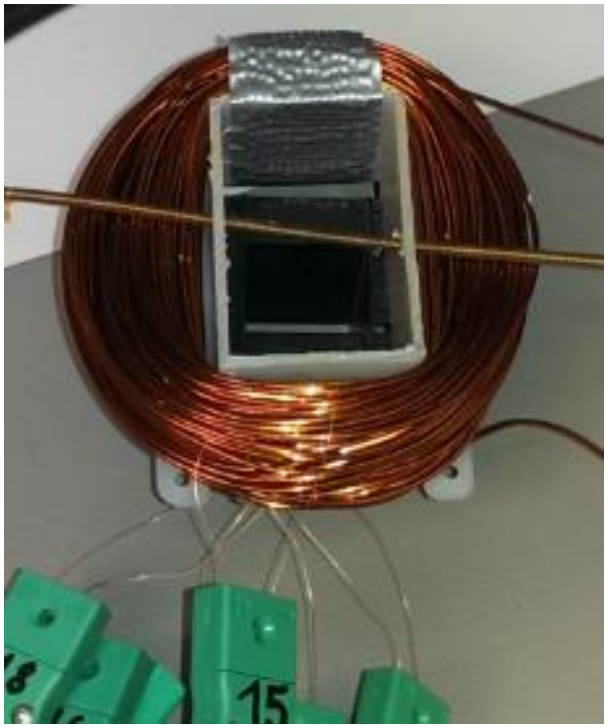

Figure 8 A2B150E Coil

Experiment 2: Single Axis Heat Transfer in Concentrated Coil

The purpose of the second experiment is to test how the heat transfer properties of the concentrated coils change when only one axis of the heat path is available. This is accomplished by using Styrofoam to thermally insulate selected portions of the coil. However, this cannot be accomplished with the round conductor coil, A2B150E, because it is not possible to isolate a single axis with a round geometry. And it is also not possible with the stator wound coil, A1S150N, because the stator apparatus obstructs the center of the coil. The three remaining coils are foil and therefore have a distinct x-, y-, and z-axis due to their rectangular structure. The z-axis is ignored because it is assumed there is no circumferential heat flow, which reduces the problem to the 2D heat flow problem (similar to the LP model that is developed in the next section, see Figure 13).

Each coil is subjected to a single operating point of 2.5 A of DC current. To study the x-axis heat transfer, Styrofoam is placed on the top and bottom of the coil, insulating the y-axis path of the coil, see Figure 9. In other words, the coil is axially insulated, only exposing the x-axis surfaces so that there is only radial heat transfer. Similarly, to study the y-axis heat transfer, the inside and outside surfaces of the coil are insulated, see Figure 10. In other words, the coil is radially insulated, only exposing the y-axis surfaces so that there is only axial heat transfer. Lastly, the plastic bobbin is removed and the coil is subjected to same DC operating point as the two single-axis experiments, see Figure 11. It is also important to note this set of three experiments is conducted for each coil in a vertical orientation, like in Figure 9 and Figure 10, and in a horizontal orientation, like in Figure 11. The vertical and horizontal orientation will affect the natural convection of the coil and having two sets of data will help to calibrate the calculated thermal resistance value for surface convection.

Radial (X-Axis) Heat Flow

As previously discussed, the x-axis heat flow experiment involved axially insulating a coil, or placing insulation on the top and bottom of the coil. This effectively removes the y-axis heat path, only permitting heat to dissipate radially through the x-axis, to the innermost or outermost layer of the coil. Styrofoam was cut to precisely cover the top and bottom of the coil. The center of the Styrofoam insulation is also removed to assure

that heat can escape from the innermost layer of the coil. The two Styrofoam blocks of insulation are fastened to the coil with zip-ties and the whole apparatus is elevated to permit natural convection evenly on all surfaces. The voltage across the coil is measured for eighty minutes in five minute increments, until the coil resistance reaches a steady state value. The resistance is calculated from the voltage and current values and used as a measure of the average temperature of the coil.

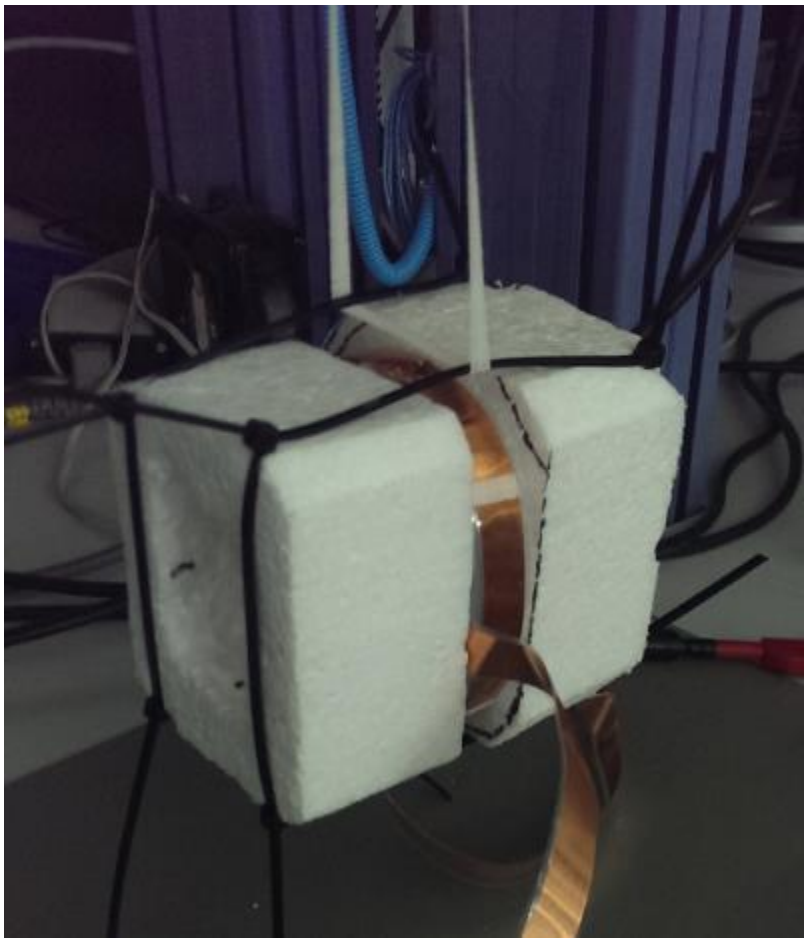

Figure 9 Single Axis Heat Transfer on X-Axis, A2B150P Coil

Axial (Y-Axis) Heat Flow

The y-axis heat flow experiment radially insulates the coil, or insulates the outside and inside of the coil, as seen in Figure 10. To truly isolate the y-axis heat path in each conductor, the x-axis heat path in each conductor would have to essentially have an infinite thermal resistance. However, this experimental setup only insulates the innermost and outermost layer of the coil, essentially making the first and last layer of

the coil to have an infinite thermal resistance in the x-direction but all the intermediate layers remain unimpeded. Therefore the y-axis heat flow experiments do not provide the intended data. Nevertheless, the setup is such that a piece of Styrofoam insulates the outside and inside of the coil, see Figure 10. Although this does not impede the x-axis thermal path for each individual winding layer, it does effectively remove the convective surfaces. This means that the only heat transfer that does occur in the x-direction is via conduction. And therefore ensures heat can only escape axially, via convection on the top and bottom of the coil, or via the y-axis.

Figure 10 Single Axis Heat Transfer for Y-Axis, A2B150N Coil

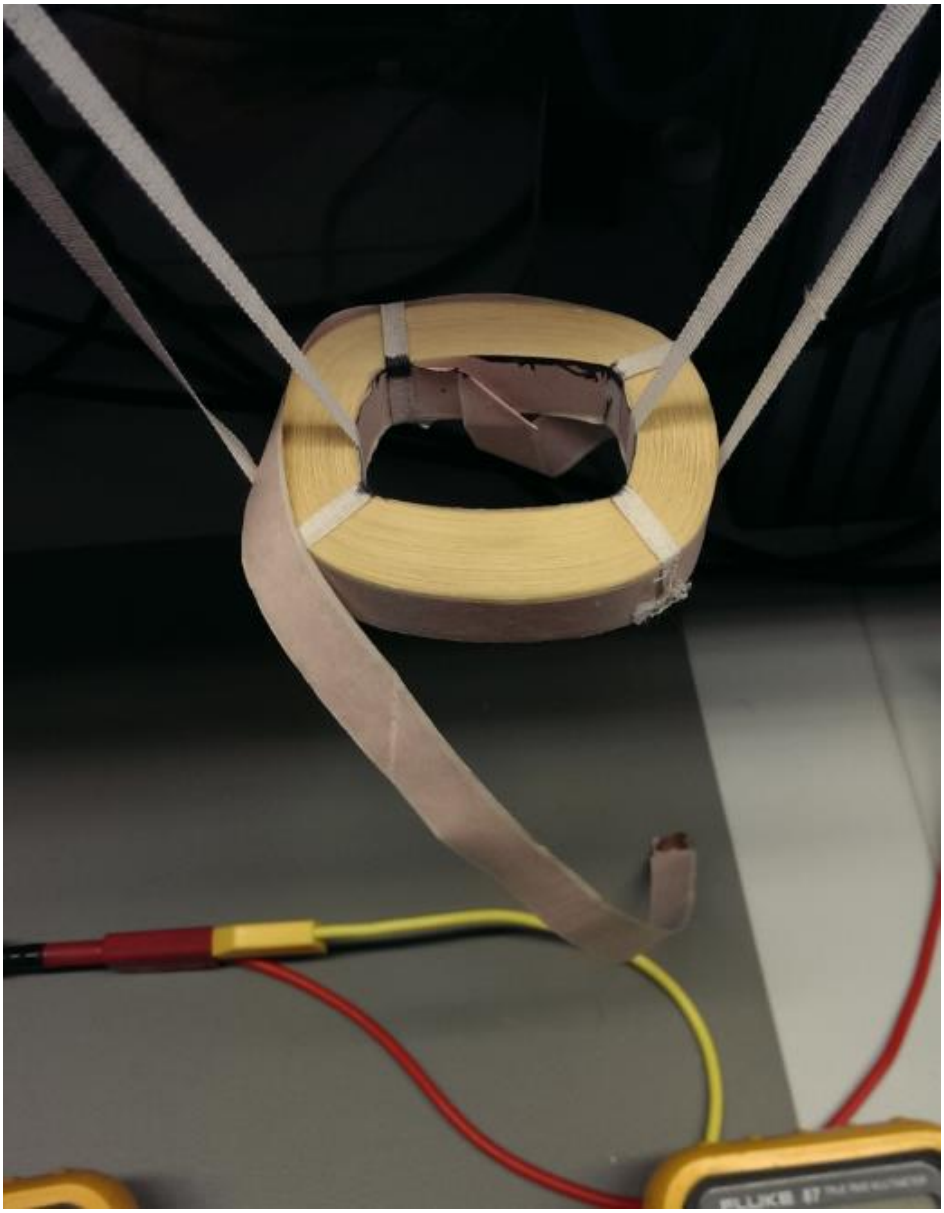

Figure 11 Coil A1B85N Horizontal Oriented without Bobbin Winding Apparatus

VI. ANALYTICAL MODEL

A LP model was developed in order to provide a fast way to determine the temperature distribution in a concentrated coil. The LP model was based on the model discussed by Mellor [16], where it is assumed that the heat flow in the x and y directions are independent, a single mean temperature per winding layer defines the heat flow, there is no circumferential heat flow, and the thermal capacity and heat generation are uniformly distributed. Due to the symmetry of the (nearly) rectangular concentrated

coils, only one length of the coil was modeled, see highlighted segment in Figure 12. And because it is assumed that there is no circumferential heat flow around the coil, the problem becomes a two dimensional heat flow problem in the XY-plane. An exaggerated view of a three turn, or three layer, coil is illustrated in Figure 13. The red dot in Figure 13 indicates the point at which the power losses are injected, which then dissipates through the thermal resistances to the ambient surrounding. The model considers the dimensions of the foil conductor and insulation, as well as the amount of air between each layer. In addition to modeling the conduction between layers, convection was added to the surface of the innermost layer, the surface of the outermost layer, and the top and bottom of each foil layer.

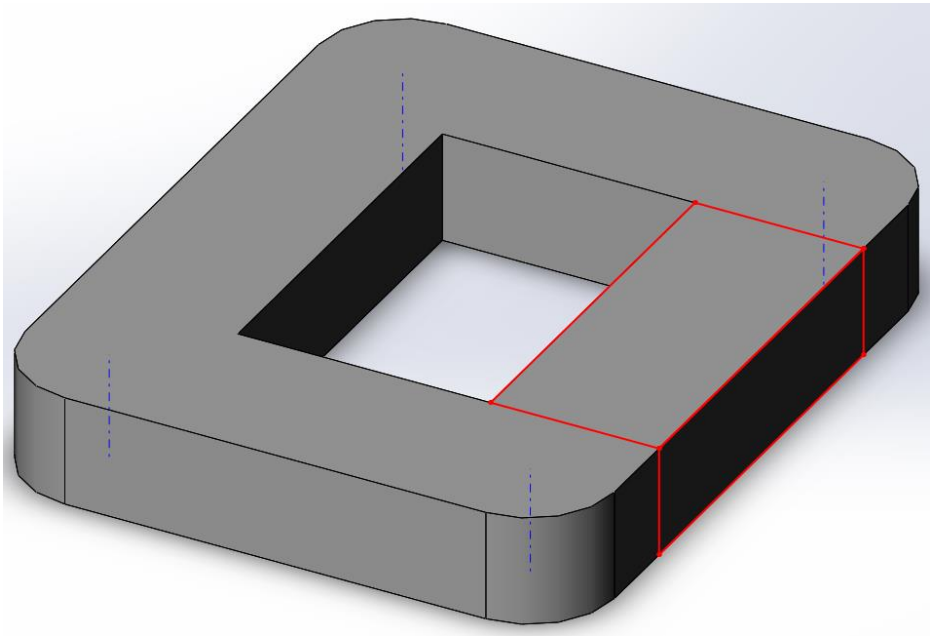

Figure 12 Highlighted Region of LP Model Segment in Concentrated Coil

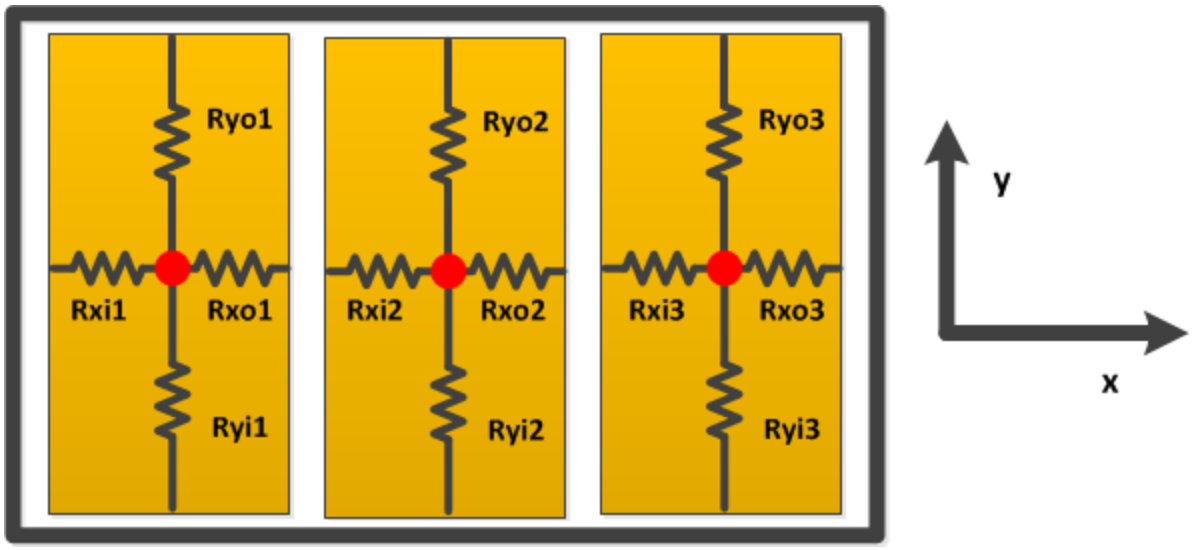

Figure 13 XY-Plane of 3 Layer LP Model Example

Three Layer Analytical LP Thermal Model Example

The following example describes the process of developing a LP thermal circuit model for a segment of rectangular conductors. This process can be expanded for any number of layers.

First, the geometry must be understood in order to know where the thermal resistances will be placed. In [16] the thermal circuit is derived for a cylindrical geometry, so the thermal resistances are placed along the radial and axial directions. In this example, the three layer model consists of three parallel rectangular conductors. As previously stated, this model assumes that heat is generated from a single point per layer; this is signified by the red dot in Figure 13. If this mean temperature point is placed at the center of each conductor and the geometry is known to be rectangular, then the placement of the thermal resistances can occur. A thermal resistance is placed along each axis (x, y, and z) and symmetric about the mean temperature point, resulting in a total of six thermal resistances per conductor. Thermal resistance is calculated by the length of the material, the inverse of the cross sectional area, and the thermal conductivity of the material. The formula to calculate the thermal resistance in the x-, y-, and z-direction are shown in equations (1), (2), and (3) respectively.

(1) $$Rxi1 = Rxo1 = \frac{Lx}{2} \cdot \frac{1}{Lz \cdot Ly} \cdot \frac{1}{k_{Cu}}$$

(2) $$Ryi1 = Ryo1 = \frac{Ly}{2} \cdot \frac{1}{Lz \cdot Lx} \cdot \frac{1}{k_{Cu}}$$

(3) $$Rzi1 = Rzo1 = \frac{Lz}{2} \cdot \frac{1}{Lx \cdot Ly} \cdot \frac{1}{k_{Cu}}$$

In order to account for the conductor insulation, the same formula is used except the thermal conductivity changes based on the insulating material. A final thermal resistance is necessary, however, in order to explain the effects of natural convection. Natural convection is a mechanism of heat transfer in which the fluid motion is not generated by an external source (e.g. a fan or pump), but only by the density differences in the fluid occurring due to temperature gradients [24]. One method that is used to represent the effects of natural convection is by using the Grashof number, which approximates the ratio of the buoyancy to viscous force acting on a fluid [25]. Since natural convection is a very complex fluid problem, analytical solutions are hard to obtain and most solutions are, therefore, empirical. There are three additional correlations that are needed to derive the thermal resistance due to natural convection, which are the Prandtl number [27], the Rayleigh number [28], and the Nusselt number [29]. The Prandtl number, like the Grashof number, is a dimensionless number defined as the ratio of the viscous diffusion rate to the thermal diffusion rate, see Equation (5) . The Rayleigh number is simply the product of the Grashof number and Prandtl number. And the Nusselt number is the ratio of the convective to conductive heat transfer across, and normal to, the surface, or boundary. It is important to note that there is a critical Grashof number, which represents the turning point from laminar heat flow over a surface to turbulent heat flow. For this experiment all of the operating points are well below the critical Grashof number so it will not be discussed further. Also, the Nusselt number will vary depending on the surface. In this case, the top and bottom of the coil segment uses the Nusselt number equations found in (9) and the inside and outside of the coil segment can be modeled as an isotherm vertical plate, as in (8). Using the known parameters to solve for the Grashof, Prandtl, Rayleigh, and Nusselt numbers, the heat transfer coefficient, h, and, consequently, the convective thermal resistance

can be determined, see Equation (10). Thus, each thermal resistor is a sum of the thermal resistance due to the copper, insulation, and convective surface; see equation (11) for an example of the total thermal resistance in the x-direction.

(4) $$Gr = \frac{buoyancy\ forces}{viscous\ forces} = \frac{g\beta\Delta TV}{\rho v} = \frac{g\beta(T_s - T_{amb})\delta^3}{v^2}$$

$$where, \quad g = gravitational\ acceleration\ \left[\frac{m}{s^2}\right]$$

$$\beta = coefficient\ of\ volume\ expansion\ \left[\frac{1}{K}\right]$$

$$\delta = characteristic\ length\ of\ the\ geometry\ [m]$$

$$v = kinematic\ viscosity\ of\ air\ at\ 300K\ \left[\frac{m^2}{s}\right]$$

(5) $$Pr = \frac{viscous\ diffusion\ rate}{thermal\ diffusion\ rate} = \frac{c_p \mu}{k}$$

$$where, \quad c_p = specific\ heat\left[\frac{J}{kg \cdot K}\right]$$

$$\mu = dynamic\ viscosity \frac{N \cdot s}{m^2}$$

$$\rho = density\left[\frac{kg}{m^3}\right]$$

(6) $$Ra = Gr * Pr$$

(7) $$Nu = \frac{Convective\ heat\ transfer}{Conductive\ heat\ transfer} = C \cdot Ra^n$$

$$where\ C\ and\ n\ depend\ on\ the\ geometry\ and\ flow$$

(8) $$Nu = 0.59 \cdot Ra^{1/4}\ for\ an\ isotherm\ vertical\ plate$$

(9) $$Nu = 0.54 \cdot Ra^{1/4}\ for\ upper\ surface\ of\ isotherm\ horizontal\ plate$$

$$Nu = 0.27 \cdot Ra^{1/4}\ for\ lower\ surface\ of\ isotherm\ horizontal\ plate$$

(10) $$h_x = \frac{Nu \cdot k_{air}}{Lx} \rightarrow R_{thermal} = \frac{1}{h_x} \cdot \frac{1}{Lz \cdot Ly}$$

(11) $$R_{Total_x} = R_{xi1} = R_{xo1}$$
$$= \left(\frac{Lx}{2} \cdot \frac{1}{Lz \cdot Ly} \cdot \frac{1}{k_{Cu}}\right) + \left(\frac{Lx}{2} \cdot \frac{1}{Lz \cdot Ly} \cdot \frac{1}{k_{insulation}}\right) + \left(\frac{1}{h_x} \cdot \frac{1}{Lz \cdot Ly}\right)$$

Next, the full thermal network is constructed, see Figure 14. Each conductor is represented by its six thermal resistances, a thermal capacitance, and a source. The ground symbols denote ambient temperature. The source represents the power losses that are injected into the node. The node, represented by θ, is the mean temperature of the conductor. In this example since the three conductors lay adjacent to each other in the x-direction, the x-axis resistors connect the three separate thermal nodes together. There are also intermediate nodes between the conductors, θ12 and θ23, which are mathematically relevant terms. The same principles to solve electrical circuits are used to solve this thermal circuit network. The linear system in equation (13) is found using Kirchhoff's circuit laws.

(12) $$\overline{G}\,\overline{V} = \overline{I} \leftrightarrow \overline{G}\,\overline{\theta} = \overline{P}_{Loss}$$
$$\Rightarrow \overline{\theta} = \overline{P}_{Loss}\ \overline{G}^{-1}$$

(13) $$\begin{bmatrix} R1 & 0 & 0 & \frac{-1}{Rzo1} & 0 \\ 0 & R2 & 0 & \frac{-1}{Rzi2} & \frac{-1}{Rzo2} \\ 0 & 0 & R3 & 0 & \frac{-1}{Rzi3} \\ \frac{1}{Rzo1} & \frac{1}{Rzi2} & 0 & -\left(\frac{1}{Rzo1} + \frac{1}{Rzi2}\right) & 0 \\ 0 & \frac{1}{Rzo2} & \frac{1}{Rzi3} & 0 & -\left(\frac{1}{Rzo2} + \frac{1}{Rzi3}\right) \end{bmatrix} \cdot \begin{bmatrix} \theta_1 \\ \theta_2 \\ \theta_3 \\ \theta_{12} \\ \theta_{23} \end{bmatrix} = \begin{bmatrix} P_{Loss1} \\ P_{Loss2} \\ P_{Loss3} \\ 0 \\ 0 \end{bmatrix}$$

$$where\ R1 = \frac{1}{Rxi1} + \frac{1}{Rxo1} + \frac{1}{Ryi1} + \frac{1}{Ryo1} + \frac{1}{Rzi1} + \frac{1}{Rzo1}$$

$$simalarly\ with\ R2\ and\ R3$$

(14) $$P_{Loss} = I^2 \cdot R_{Coil}\left(\frac{1}{N} \cdot \frac{L_{coil\ segment}}{L_{coil}}\right)$$

The only unknown variable in this particular experiment is the mean temperature vector, or the θ vector, as seen in (12). The power loss injection, P_{Loss}, is known because a DC constant current source is the sole contributor to the thermal losses. Note that the resistance of the coil must be scaled by the number of turns and ratio of the coil segment, see equation (14). The thermal capacitances can be ignored since it is a steady state thermal experiment. Solving for the mean temperature vector, θ, results in the mean temperature of every layer of the coil segment.

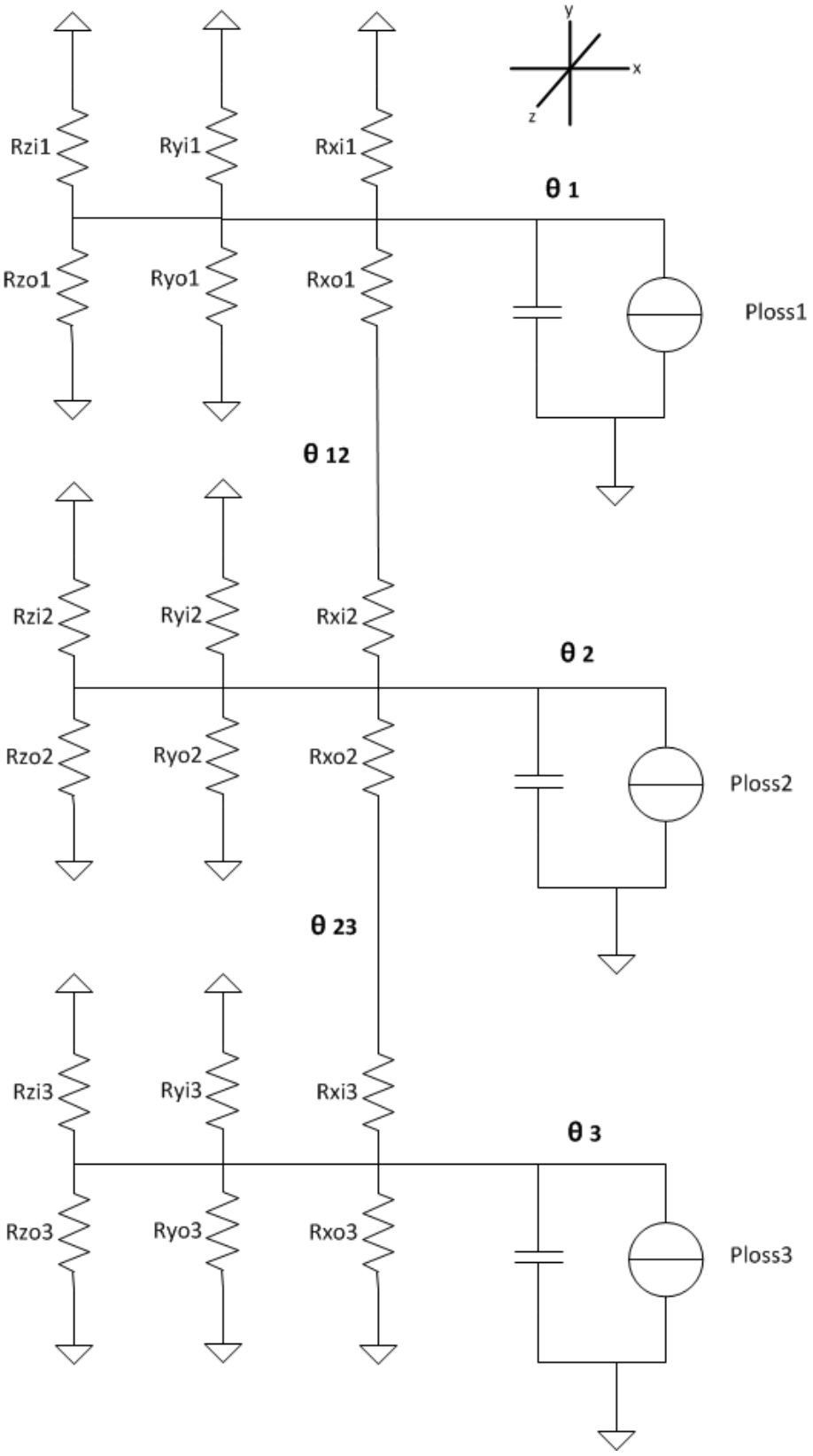

Figure 14 Thermal Circuit of 3 Layer Example

VII. RESULTS

Several authors have claimed that foil windings have better thermal characteristics than their round conductor counterparts. This section presents observations about the steady state thermal behavior of the five concentrated coils begins to understand the design trade-offs that are implied by these observations.

Observation 1: LP Model Predicts Temperature Distribution in Foil

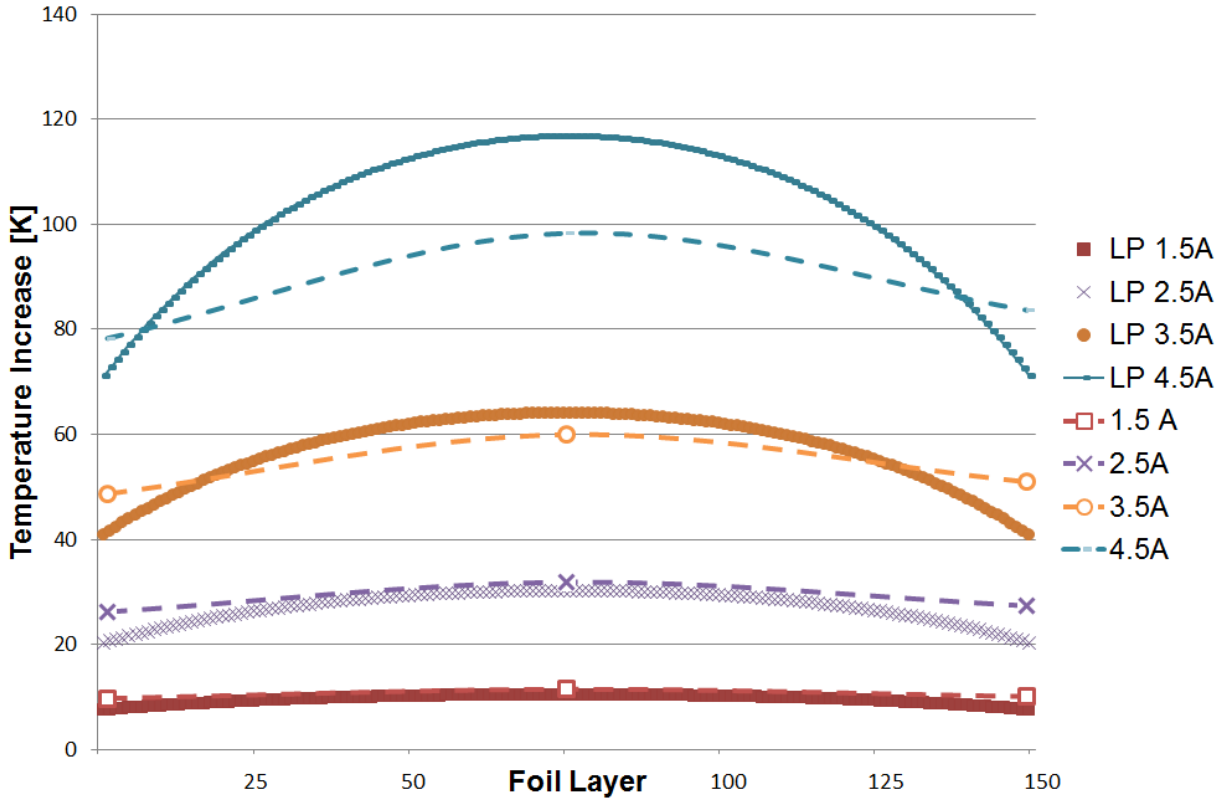

Figure 15 Coil A2B150P LP vs Measured Temperature Distribution

The analytical LP thermal model described in the previous section develops a thermal circuit model for a segmented portion of a foil wound concentrated coil. Figure 15 illustrates how the LP model accurately represents the inverted-U shape temperature distribution in the foil windings. This particular graph includes the temperature distribution across 150 layers of the foil windings at four operating points, 1.5, 2.5, 3.5, and 4.5 A DC. The LP thermal model actually provides the mean temperature for every single layer, whereas the measured temperature values are recorded at only three distinct points. For comparison, the measured results for the same coil are included,

which can be identified by the dotted lines. The rounded profile indicates that there is indeed a hot spot at the middle layers of the foil coil segment. However, it will become clearer in the later observations that one advantage of using foil is that it can transfer heat to outside layers very effectively.

Observation 2: Foil Conductor vs Round Conductor

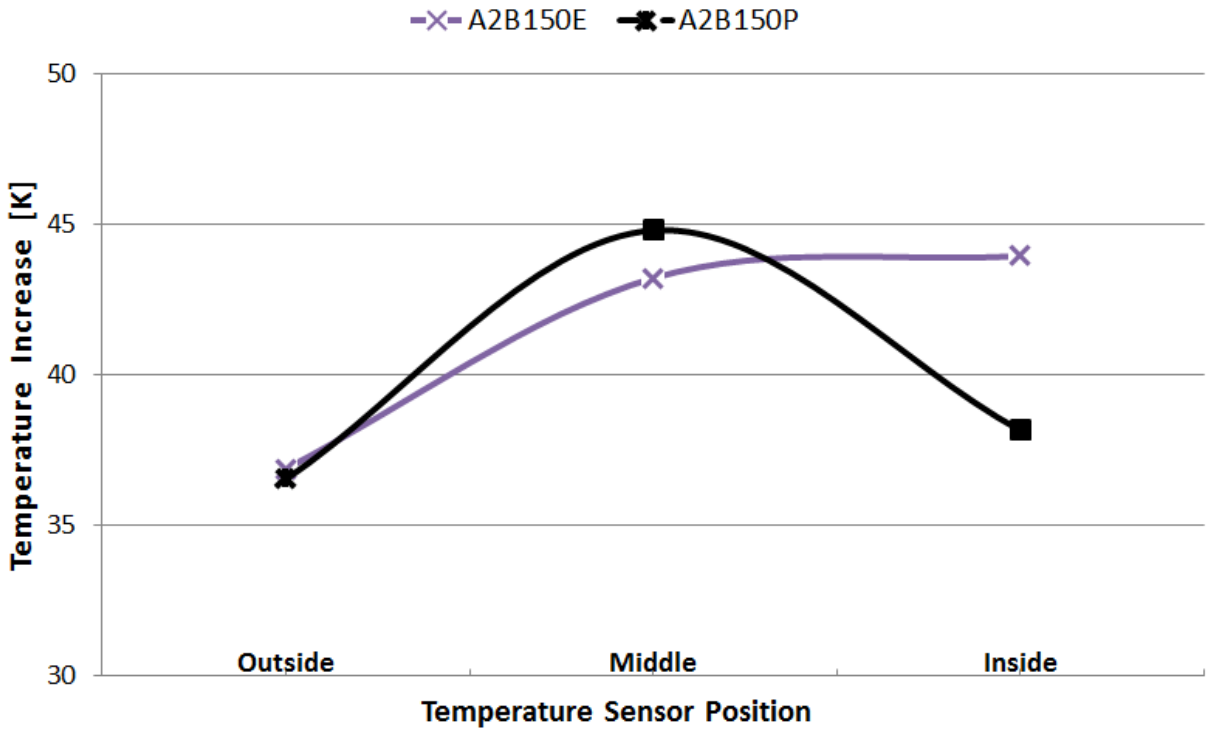

Figure 16 Coil A2B150E and A2B150P Temperature Distribution at 3A DC

The main feature to observe in Figure 16 is the overall temperature distribution. The single-sided PET insulated foil wound coil, coil A2B150P, is indicated in black and the baseline round conductor coil is indicated in purple. In this case both coils were subjected to 3 A DC and the steady state temperature was recorded from the thermistors embedded in each coil. The foil wound coil, A2B150P, exhibits the predicted inverted-U shape. In contrast the round conductor wound coil, A2B150E, has an increasing temperature distribution so that the inside temperature exceeds even the midpoint temperature. This feature is unique only to round conductor coil, A2B150E. And although the midpoint temperature of coil A2B150E is lower than coil A2B150P the overall temperature distribution in the foil wound coil is much better. The inverted-U

shape that the foil wound coils exhibit can be attributed to the large surface area of the first and last layer of the coil, which more effectively facilitates natural convection heat transfer. The inside and outside of coil A2B150E is segmented by the smaller geometry of the round conductors and therefore cannot transfer heat as effectively. A bundle of round conductors only contact the adjacent round conductor at a single point. So the most efficient means of heat transfer, conduction, is limited to the single point of contact between the round geometries. Whereas, a foil type geometry facilitates a far superior heat transfer profile because there is a large surface area contact between layers.

Observation 3: Double-Sided Nomex Paper Insulation vs Single-Sided PET Insulation

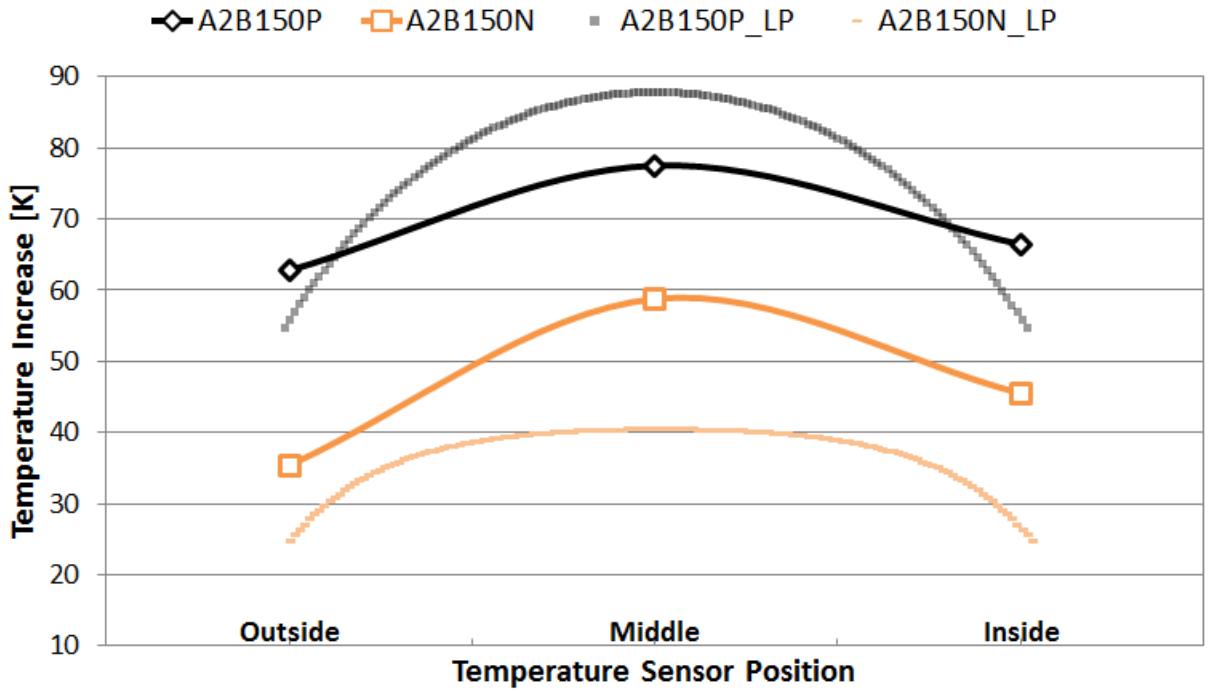

Figure 17 Coil A2B150P and A2B150N Temperature Distribution at 4A DC

Coil A2B150P and A2B150N are compared here to show that for an identical DC current input and power loss (14.3 W) there is still a distinct difference between the two temperature distributions. Coil A2B150N has more than twice the amount of insulation as coil A2B150P since it has double-sided insulation and the Nomex paper is thicker than the PET film. The excessive amount of insulation shows the limit of the LP model. Since coil A2B150N contains so much more insulation the volume of the coil is much

larger than any of the other investigated coils. It is so large that the overall shape of the coil appears more circular than rectangular, see Figure 10. This discrepancy is evident in the results presented in Figure 17. Notice that the discrepancy between the measured results for coil A2B150N and the expected LP results are far greater than the discrepancy found in coil A2B150P. Coil A2B150P provides more than enough insulation for applications in electric machines and is more easily modeled via the proposed LP thermal model. Of course, the LP thermal model is limited even in the scope of coil A2B150P, particularly at higher input current values. This will be an area of focus for future work.

Observation 4: Foil on Stator vs Round Conductor on Bobbin

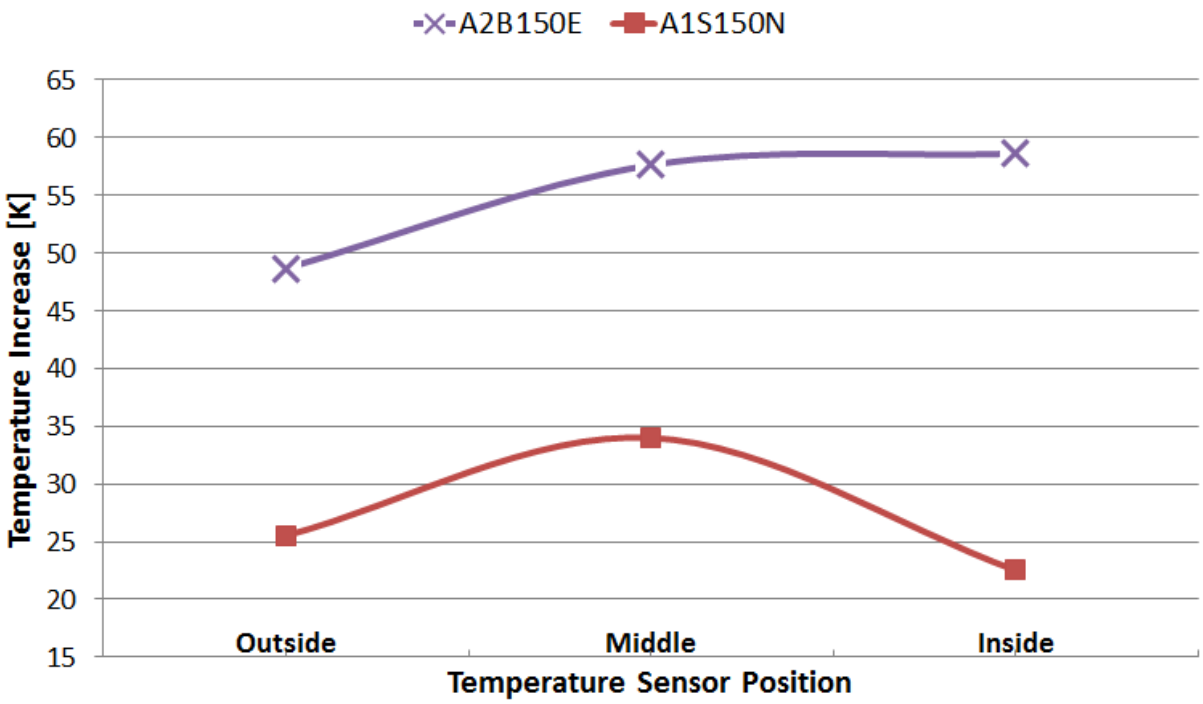

Figure 18 Coil A2B150E and A1S150N Temperature Distribution at $P_{Loss} \approx 9.5$ W

Although this study of foil wound concentrated coils evolved from an ironless stator design it is much more common for concentrated coils to be wound around plastic bobbins and placed on fixed iron stator teeth. Therefore it was important to investigate foil wound concentrated coils placed directly on a stator tooth. Removing the need for a plastic bobbin to contain the concentrated coil on the stator tooth is very advantageous because it effectively removes a large thermal insulator between the coil and the stator

teeth. And stator teeth will generally have a direct thermal path to ambient per the motor frame. Coil A2B150E is at power loss of 8.77 W and coil A1S150N is at power loss of 10.053, resulting in a 12.8% difference. Therefore, it is evident by Figure 18 that a foil wound concentrated coil directly on a stator tooth transfers heat much more efficiently than a round conductor wound concentrated coil on a plastic bobbin with the same power loss injection. The average temperature of the foil wound coil on the stator is approximately 25 degrees Kelvin lower than the round conductor coil. Another feature to note is that the outside temperature sensor is slightly higher than the inside temperature sensor for coil A1S150N because the stainless steel in the center of the coil provides a better thermal path for the coil. It is this better thermal path that is responsible for the much lower average temperature and the inward skew of the temperature distribution of coil A1S150N.

Observation 5: Stator Apparatus vs Plastic Bobbin

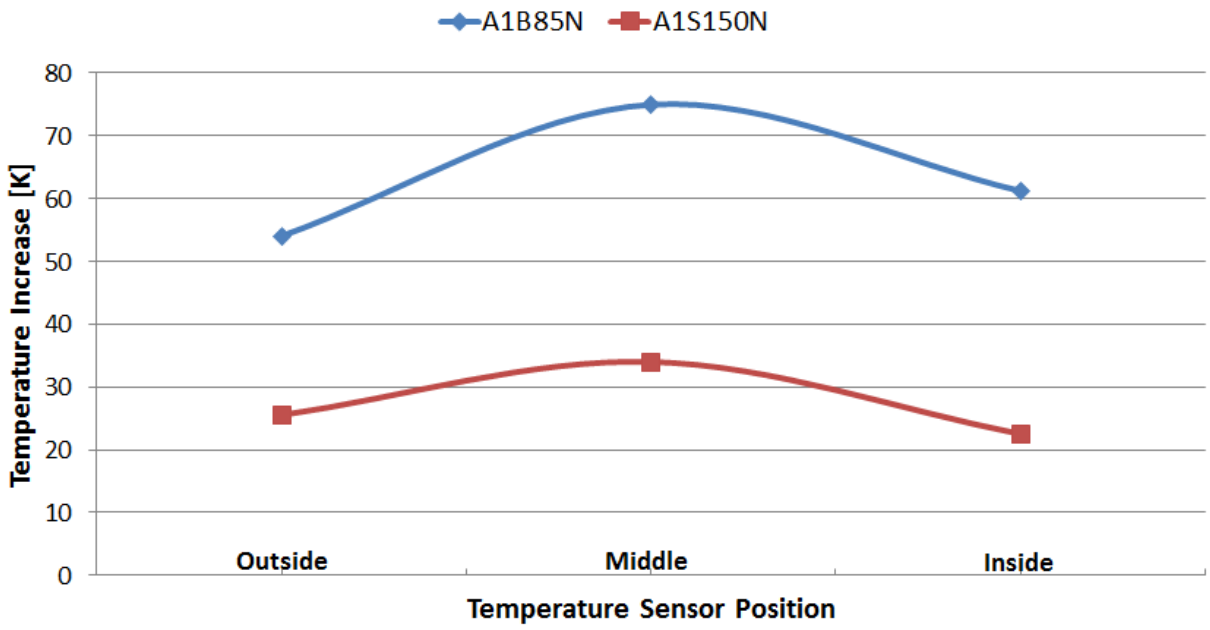

Figure 19 Coil A1B85N and A1S150N Temperature Distribution at $P_{Loss} \approx 10$ W

From a theoretical standpoint, the temperature distribution of adjacent rectangular conductors should peak in the middle but be equal on inside and outside layer. However, all the coils that are wound around a plastic bobbin, indicated by a “B” in the coil name, have a slightly higher temperature on the inside temperature sensor

compared to the outside sensor. This skew in the temperature distribution is because the plastic bobbin partially impedes natural convection from the inside layer. Additionally, the plastic bobbin adds a large thermal resistance to any coil. Also, it is known from the previous observation that a foil wound concentrated coil has the advantage of being able to be directly placed on a stator tooth without the need of a plastic bobbin to maintain its structure. Figure 19 illustrates the skew of the temperature distribution for coil A1B85N, toward the outside temperature sensor, and coil A1S150N, toward the inside temperature sensor. Coil A1B85N is at a power loss of 10.692 W and coil A1S150N is at a power loss of 10.053, resulting in a 6.4% difference. So both coils have the same conductor cross section area and same power loss injection, yet coil A1S150N has an average temperature approximate 35 degrees Kelvin lower than coil A1B85N around the plastic bobbin. To reiterate from the last observation, the stator apparatus provides a superior thermal path from coil A1S150N to remove heat. This is evident by the lower overall temperature of coil A1S150N and the inward skew of the temperature distribution.

Observation 6: Vertical vs Horizontal Coil Orientation

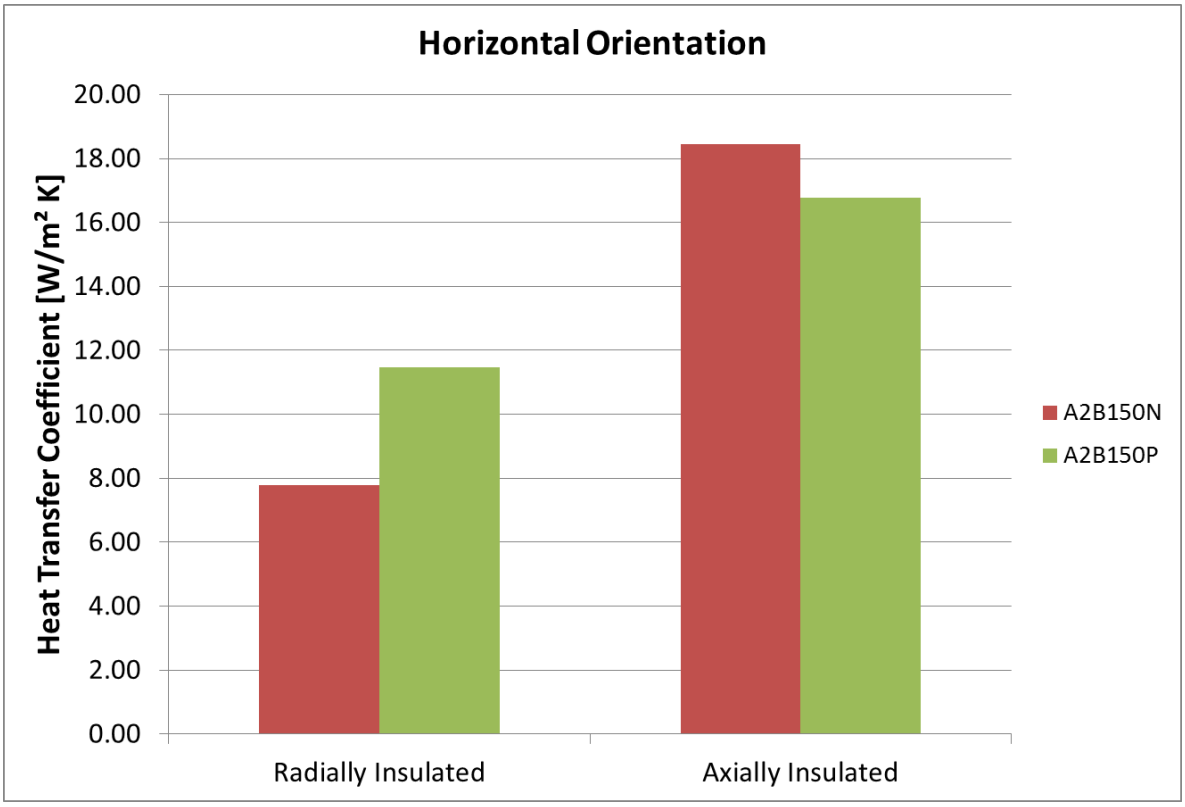

Figure 20 Coil A2B150P and A2B150N Heat Transfer Coefficient, Horizontal Orientation

The intent of the second experiment was to study the heat transfer properties of the concentrated coils in a single axis. This is achieved by radially insulating the coil to study the axial heat transfer, or y-axis, and by axially insulating the coil to study the radial heat transfer, or x-axis. In both cases in this experiment, it was possible to measure the surface area exposed thus providing a quantitative measure of the axial and radial surface area for each coil. It is also possible to extract the average temperature for each coil based on the linear relationship between temperature and the resistance of the coil. The power loss injected in each coil is also known because the second experiment is performed at a constant 2.5A. Therefore, it is possible to calculate the heat transfer coefficient for each coil in the axial and radial directions. Figure 20 shows that the heat transfer is much better in the radial direction for both coils. Coil A2B150N can transfer heat more than 2 times more efficiently in the radial direction than in the axial direction. This result is key to explaining the advantage of foil conductors over round conductors, which is that the large surface area of the foil

conductor permits much better heat transfer. This idea supports Observation 2 that the large surface area of the foil conductors can transfer heat to the boundaries of the concentrated better than a bundle of round conductors can. From a theoretical perspective a bundle of round conductors only make contact with one another at a single point. It is at this single point where heat can conduct from one round conductor to the next. Foil conductors have full contact between layers in the radial direction to facilitate conduction of heat to the ambient boundaries.

Summary

Observation 1 illustrates the inverted-U shape temperature distribution for foil wound concentrated coils as predicted by the LP thermal model. Observation 2 discusses the overall temperature distribution advantage that foil wound concentrated coils have over their round conductor counterpart. Observation 3 shows that using double-sided Nomex paper insulation distorts the shape of the concentrated coil enough to deviate far from the predicted LP model results. Observation 4 demonstrates an advantage of using foil wound concentrated coils is that they can be placed directly on a stator tooth without the need for a plastic bobbin to maintain its structure. Observation 5 supports the previous observation because it shows that placing a foil wound concentrated coil directly on a stator tooth provides a superior thermal path for heat to transfer to ambient via the stator structure. Observation 6 highlights the superior radial heat transfer in foil windings due to the large surface of the adjacent layers. These observations provide quantitative evidence that foil wound concentrated coils indeed have superior steady state thermal characteristics when compared to the standard round conductor wound concentrated coil.

VIII. CONCULUSIONS AND FUTURE WORK

This study of foil wound concentrated coil stemmed from an impressive study conducted by Melendez-Vega [1] utilizing Aluminum foil prototype concentrated coils which performed near their baseline copper counterpart. Foil conductors are much more commonly found in inductors or transformers but there have been several studies in the literature that indicate a niche for nontraditional winding geometries for use in electric machines. This study provides a detailed analysis of the steady state heat transfer

characteristics of foil wound concentrated coils. It was found that there are distinct advantages that foil conductors have over their round conductor counterpart. The rectangular geometry of the foil conductors not only promotes a fast, accurate LP thermal model but also a large surface area for heat conduction between layers in a concentrated coil. Additionally, foil wound concentrated coils have the advantage that they can be placed directly on a stator tooth, which removes the thermally insulating plastic bobbin from the design and provides a clear thermal path to the metallic stator tooth structure.

There are many lessons learned from this study that will aid in the remaining experiments needed to complete a detailed study of foil wound concentrated coils. One-sided insulation is more than enough considering the application for the foil wound concentrated coils is in electric machines where voltage levels are well below the voltage breakdown of PET. It is important to make sure that the future coils to be investigated are chosen to be practical test subjects. For example, it is important to find a variation of a foil winding with enamel insulation to add to the next round of experiments. And even anodized aluminum, following the study in [9], can be considered a strong candidate for an additional coil variation. An improved LP thermal model is absolutely necessary, especially as the power loss injection increases. It can be seen in Figure 15 that nonlinearities must begin to occur at higher current values since the measured and expected temperature distributions begin to diverge. Perhaps some of the assumptions made to construct the LP model described will not suffice at these higher input current values. It may be necessary to consider that the outside layers of a concentrated coil have a larger resistance than the inside layers. Such imbalances may not permit the assumption that there is no circumferential heat flow in a concentrated coil. The property of thermal expansion is also not considered in the thermal model, which surely plays a role at higher temperatures. It is also important to understand how the boundary conditions of the coil under test especially when making thermal measurements because this can greatly affect the behavior of the predicted coil temperature distribution. A well-defined boundary could also have a great impact on the accuracy of the LP thermal model. Many of the referenced studies had known boundary conditions, which would certainly be an improvement to the natural convection

approximations used. Accurate thermal measurements are not a trivial and proper equipment and attention to detail are necessary for the success of future thermal experiments.

Future Work - Preliminary Exam Outline

One final task for the Marshall Plan Scholarship was to create an outline for the upcoming Preliminary Exam. At the University of Wisconsin the Preliminary exam is a detailed exam covering the proposed research leading to the final Ph.D. dissertation. This is an important step because it provides an outline for the next steps of this research topic. A thorough study of foil wound concentrated coils must be completed and Table 2 provides a framework for the comprehensive study. This Marshall Plan Scholarship has provided the time and resources necessary to complete two of the four more important tasks involved in the completion of this dissertation, the DC Losses in Foil Windings and Analytical Thermal Model. Much of the first Introduction section was also completed as a result of this report.

The immediate next step is to begin the study of the AC Losses in foil windings, which was alluded to in the AC Losses section of the literature review. This is a very important next step and crucial to the justification of using foil conductors in electric machines. New coil candidates will be introduced. The thermal model will be improved to address the nonlinearities that occur at higher input current levels. Proper thermal chambers will be used to conduct any further thermal experiments to promote known boundary conditions on any device under test. The final dissertation study will culminate with an implementation of foil windings in an electric machine environment that exploits the advantages of the foil geometry. The final machine will prove that foil windings can be utilized to increase the torque per amp rating, due to their superior thermal characteristics. This implies a higher torque density for a given machine and possibly permits the use of alternative metals to be used as machine windings. Creating framework to allow for the use of more sustainable metals, like aluminum, in electric machines is very important considering the growing prevalence of electric machines in industry and everyday life.

Table 2 Preliminary Exam Outline

I) Introduction
- *a. Background and Statement of Problem*
- *b. Purpose of Research Thesis Program*
- *c. Literature Review on Foil Windings*
- *d. Literature Review on AC Losses*
- *e. Literature Review on Analytical Thermal Models*
- *f. Organization of Thesis*

II) DC Losses in Foil Windings
- *a. Heat Transfer in Foil Wound Concentrated Coils*

III) AC Losses in Foil Windings
- *a. Skin Effect Losses*
- *b. Proximity Losses*

IV) Analytical Thermal Model for Foil Wound Concentrated Coils
- *a. Lumped Parameter Model*
- *b. Finite Element Model*

V) Machine Design for Foil Windings
- *a. Machine Specifications*
- *b. Machine Design Development*
- *c. Machine Loss Analysis and Reduction*
  - *i. Overview*
  - *ii. DC Winding Losses*
  - *iii. AC Winding Losses*
  - *iv. Iron Losses*
  - *v. Magnet Losses*
- *d. Machine Fabrication*
- *e. Finite Element and Analytical Models*

VI) Conclusions and Future Work
- *a. Conclusions on Foil Windings*
- *b. Key Technical Contributions*
- *c. Future Work*

VII) References

VIII) Appendix
- *a. Lumped Parameter Thermal Models*
- *b. Skin Effect Models*
- *c. Dyno Setup*
  - *i. Description of Dynamometer*
  - *ii. Generator Machine and Drive*
  - *iii. Torque Meter Calibration*
  - *iv. Current Sensor Calibration*
  - *v. Power Meter Setup*
- *d. Machine Setup*

IX. ACKNOWLEDGEMENTS

I would like to express my gratitude to Professor Giri Venkataramanan for facilitating this wonderful research opportunity, the Marshall Plan Foundation for their financial support, and especially to Professor Mütze and the EAM staff for all of their support and the warm welcome to Austria.

X. REFERENCES

[1] Melendez-Vega, Pedro. “Design of Tube-Based Blades and Aluminum-Foil-Wound Coils for Human Scale Wind Turbines.” M.S. Thesis, University of Wisconsin - Madison, 2012.

[2] Reed, Justin. “Modeling of Battery-Charging Turbines.” M.S. Thesis, University of Wisconsin - Madison, 2008.

[3] H. Piggott. How to build a wind turbine. Hugh Piggott: Scotland, 2005. http://www.scoraigwind.com

[4] Kamper, Maarten, Rong-Jie Wang, and Francois Rossouw. “Analysis and Performance of Axial Flux Permanent-Magnet Machine With Air-Cored Nonoverlapping Concentrated Stator Windings.” IEEE Transactions on Industry Applications 44, no. 5 (2008): 1495–1504.

[5] Arumugam, P., T. Hamiti, and C. Gerada. “Modeling of Different Winding Configurations for Fault-Tolerant Permanent Magnet Machines to Restrain Interturn Short-Circuit Current.” IEEE Transactions on Energy Conversion 27, no. 2 (June 2012): 351–61. doi:10.1109/TEC.2012.2188138.

[6] Arumugam, P., T. Hamiti, C. Brunson, and C. Gerada. “Analysis of Vertical Strip Wound Fault-Tolerant Permanent Magnet Synchronous Machines.” IEEE Transactions on Industrial Electronics 61, no. 3 (March 2014): 1158–68. doi:10.1109/TIE.2013.2259777.

[7] Shea, Adam, and Dan Ludois. “Reduction of Permanent Magnets in Small-Scale Wind Turbines.” IEEE Energy Conversion Congress and Exposition (ECCE), n.d., 5105–11.

[8] Lorilla, L.M. “Foil Field Lundell Alternator with Rotating Power Electronics.” IEEE Power Electronics Specialists Conference, June 18, 2006, 2164–69.

[9] Babicz, S., S.A.-A. Djennad, and G. Velu. “Preliminary Study of Using Anodized Aluminum Strip for Electrical Motor Windings.” In 2014 IEEE Conference on Electrical Insulation and Dielectric Phenomena (CEIDP), 176–79, 2014. doi:10.1109/CEIDP.2014.6995808.

[10] Lomheim, Sigbjorn. “Analysis of a Novel Coil Design for Axial Flux Machines.” M.S. Thesis, Norwegian University of Science and Technology, 2013.

[11] Boglietti, A., A. Cavagnino, and D. Staton. “Determination of Critical Parameters in Electrical Machine Thermal Models.” IEEE Transactions on Industry Applications 44, no. 4 (July 2008): 1150–59. doi:10.1109/TIA.2008.926233.

[12] Boglietti, A., A. Cavagnino, D. Staton, Martin Shanel, M. Mueller, and C. Mejuto. “Evolution and Modern Approaches for Thermal Analysis of Electrical Machines.” IEEE Transactions on Industrial Electronics 56, no. 3 (March 2009): 871–82. doi:10.1109/TIE.2008.2011622.

[13] Staton, D., A. Boglietti, and A. Cavagnino. “Solving the More Difficult Aspects of Electric Motor Thermal Analysis in Small and Medium Size Industrial Induction Motors.” IEEE Transactions on Energy Conversion 20, no. 3 (September 2005): 620–28. doi:10.1109/TEC.2005.847979.

[14] Bousbaine, Amar. “Investigations of Thermal Modelling of Induction Motors.” Ph.D. Dissertation, University of Sheffield, 1993.

[15] Okoro, O.I. “Steady and Transient States Thermal Analysis of a 7.5-kW Squirrel-Cage Induction Machine at Rated-Load Operation.” IEEE Transactions on Energy Conversion 20, no. 4 (December 2005): 730–36. doi:10.1109/TEC.2005.852965.

[16] Mellor, P.H., D. Roberts, and D.R. Turner. “Lumped Parameter Thermal Model for Electrical Machines of TEFC Design.” IEE Proceedings 138, no. 5 (September 1991): 205–18.

[17] Simpson, N., R. Wrobel, and P.H. Mellor. “Estimation of Equivalent Thermal Parameters of Impregnated Electrical Windings.” IEEE Transactions on Industry Applications 49, no. 6 (November 2013): 2505–15. doi:10.1109/TIA.2013.2263271.

[18] Wrobel, R., and P.H. Mellor. “A General Cuboidal Element for Three-Dimensional Thermal Modelling.” IEEE Transactions on Magnetics 46, no. 8 (August 2010): 3197–3200. doi:10.1109/TMAG.2010.2043928.

[19] Kheraluwala, Mustansir, Donald Novotny, and Divan Deepakraj. “Coaxially Wound Transformers for High Freq High Power.” IEEE Transactions on Power Electronics 7, no. 1 (January 1992): 54–62.

[20] Zhang, Wanjun, and T.M. Jahns. “Analytical 2-D Slot Model for Predicting AC Losses in Bar-Wound Machine Windings due to Armature Reaction.” In 2014 IEEE Transportation Electrification Conference and Expo (ITEC), 1–6, 2014. doi:10.1109/ITEC.2014.6861825.

[21] Wojciechowski, Rafal M., and Cezary Jedryczka. “The Analysis of Stray Losses in Tape Wound Concentrated Windings of the Permanent Magnet Synchronous Motor.” COMPEL: The International Journal for Computation and Mathematics in Electrical and Electronic Engineering 34, no. 3 (January 16, 2015): 766–77.

[22] Lammeraner, Jiri, and Milos Stafl. Eddy Currents. Iliffe Books Ltd, London, 1966.

[23] “Comparison of Thermocouples, RTDs, and Thermistors.” Sensory Embedded Electronics, Accessed 27 Aug 2015, http://www.sensoray.com/support/appnotes/thermocouples_rtds_thermistors.htm

[24] “Natural Convection.” Wikipedia, Last modified 24 August 2015, https://en.wikipedia.org/wiki/Natural_convection

[25] Bahrami, M. “Natural Convection.” ENSC 388 Lecture Notes. Simon Fraser University, September 2009.

[26] Grashof Number.” Wikipedia, Last modified 24 August 2015, https://en.wikipedia.org/wiki/Grashof_number

[27] Prandtl Number.” Wikipedia, Last modified 18 August 2015, https://en.wikipedia.org/wiki/Prandtl_number

[28] Rayleigh Number.” Wikipedia, Last modified 29 May 2015, https://en.wikipedia.org/wiki/Rayleigh_number

[29] Nusselt Number.” Wikipedia, Last modified 1 September 2015, https://en.wikipedia.org/wiki/Nusselt_number